Materials Science in Semiconductor Processing 59 (2017) 35–39

Contents lists available at ScienceDirect

Materials Science in Semiconductor Processing

journal homepage: www.elsevier.com/locate/mssp

Influence of in-situ SiN_x mask on the quality of N-polar GaN films

Long Yan, Yuantao Zhang*, Heng Xu, Ling Li, Junyan Jiang, Zhen Huang, Xu Han, Junfeng Song, Guotong Du

State Key Laboratory on Integrated Optoelectronics, College of Electronic Science and Engineering, Jilin University, Qianjin Street 2699, Changchun 130012, People's Republic of China

A R T I C L E I N F O

Keywords:
SiN_x insertion
GaN
N polar
MOCVD

A B S T R A C T

We utilized in-situ grown SiN_x insertion mask to improve the quality of N-polar GaN films on sapphire substrates by metal-organic chemical vapor deposition. The influences of deposition time and position of SiN_x insertion mask were studied. Under the optimal SiN_x mask growth conditions, the full width at half maximum values of (0002) and (10$\bar{1}$2) XRD rocking curves of N-polar GaN films are decreased to 88″ and 172″, respectively. Simultaneously, Raman spectroscopy measurements reveal that SiN_x mask can also reduce the tensile residual stress of N-polar GaN films. In addition, the electrical and optical properties of N-polar GaN films with and without SiN_x insertion mask were investigated by temperature dependent Hall and photoluminescence measurements. It is found that N-polar GaN film with SiN_x insertion mask has lower background carrier concentration, higher mobility and lower nonradiative recombination rate.

1. Introduction

GaN and its In and Al alloys are widely used in light emitting diodes, laser diodes, and electronic devices due to their superior physical properties. Because of the polar asymmetry, the films grown along the c-axis have two different polarities, Ga-polar (0001) and N-polar (000$\bar{1}$). So far, the majority of nitride devices are based on Ga-polar GaN. N-polar GaN attracts more and more attention recently because its unique advantages in some respects over Ga-polar GaN. For example, N-polar LEDs have potential in mitigating efficiency droop because they can provide a higher potential barrier against carrier overflow [1]. Enhanced indium incorporation into N-polar InGaN films was observed as compared to the corresponding Ga-polar InGaN [2]. In addition, N-polar GaN high-electron-mobility transistors with enhancement mode operation have been reported [3]. However, the development of N-polar devices is limited by its poor crystal quality. The defects density, such as the density of threading dislocations (TDs) and the concentration of oxygen impurity, is typically higher than that of Ga-polar GaN [4,5]. Epitaxial lateral overgrowth (ELOG) is a suitable technique for improving the quality of epitaxial films, which has been proved in Ga-polar GaN [6,7]. Recently, Song et al. also applied ELOG technique successfully in N-polar GaN by using SiO_2 as the mask [8]. In this study, we used in-situ deposited SiN_x as the mask of ELOG to improve N-polar GaN films quality. By optimizing the deposition time and position of SiN_x insertion mask, TDs density and residual stress of GaN films decrease significantly. In addition, N-polar GaN films with the optimized SiN_x insertion mask demonstrate lower background carrier concentration, higher mobility and lower nonradiative recombination rate.

2. Experiments

Unintentionally doped N-polar GaN films were grown on sapphire substrate by using AIXTRON CCS 3×2″ FT MOCVD system. The growth process is described as follows. After cleaned in H_2 atmosphere for 5 min at 1100 °C, sapphire substrate was nitrided at 1060 °C in a mixture of NH_3 (2 slm) and N_2 (6 slm) for 180 s. A ~10 nm thick GaN buffer was grown at 560 °C by using Triethylgallium (TEGa) and NH_3. Then, 2 μm thick N-polar GaN film with SiN_x mask was grown at 1080 °C using trimethylgallium (TMGa) as group III source. SiN_x was in-situ inserted using silane (SiH_4) and NH_3 at 1050 °C during the interruption of GaN growth. Two series of GaN films with same thicknesses were grown with different inserted deposition times and positions of SiN_x. In series I, SiN_x mask was inserted after the growth of 300 nm thick GaN. The deposition times of SiN_x varied from 30 s to 180 s. In series II, the position of SiN_x mask was changed. The SiN_x masks were inserted after the growth of 100 nm, 300 nm and 500 nm GaN, respectively. For comparison, N-polar GaN without SiN_x mask was also prepared, named as Sample A. The polarity of GaN film was ascertained by wet etching with KOH solution (8 mol/L) for 10 min at

* Corresponding author.
E-mail address: zhangyt@jlu.edu.cn (Y. Zhang).

http://dx.doi.org/10.1016/j.mssp.2016.11.034
Received 15 August 2016; Received in revised form 16 November 2016; Accepted 20 November 2016
Available online 03 December 2016
1369-8001/

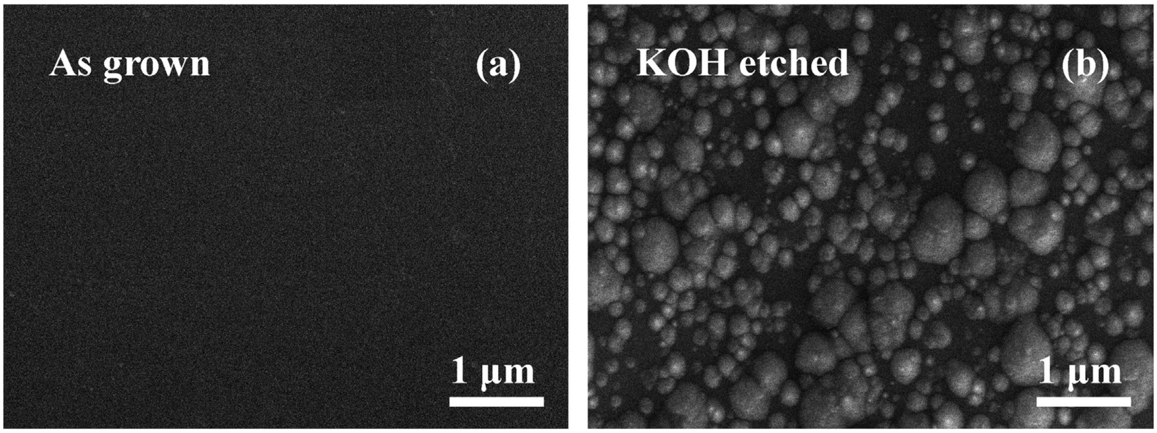

Fig. 1. SEM images of the surface morphologies of as grown (a) and KOH etched (b) N-polar GaN films with SiN_x insertion mask.

40 °C. The surface morphology was characterized by field emission scanning electron microscopy (SEM; Jeol-7500F). X-ray diffractometer (XRD; Rigaku Ultima IV) and Raman spectroscopy (Renishaw, inVia) were used to examine the crystallinity and stress, respectively. The electrical properties of GaN films with and without SiN_x insertion mask were investigated by Hall effect measurements (ACCENT HL5500PC, UK). The Ohmic contacts were processed by using indium metal combined with rapid thermal annealing. The optical properties were investigated by photoluminescence (PL) measurements with a He–Cd laser (325 nm, 25 mW) as an excitation source.

3. Results and discussion

Fig. 1 shows the surface SEM images of as-grown and KOH etched N-polar GaN films with SiN_x insertion mask. Compared with the smooth surface of the as-grown film shown in Fig. 1(a), hexagonal pyramids are observed on the surface of the etched film in Fig. 1(b). It has been demonstrated that the reaction to KOH solution occur only on N-polar GaN [9]. This indicates that GaN films with SiN_x mask are still N-polar and SiN_x insertion mask does not induce polarity inversion.

Fig. 2(a) shows the full width at half maximum (FWHM) values of XRD rocking curves of (0002) and ($10\bar{1}2$) planes of GaN in series I. Zero point on horizontal axis represents the deposition time of SiN_x mask is 0 s. When SiN_x deposition time increases to 30 s, the FWHM values of (0002) and ($10\bar{1}2$) reduce significantly from 144″ and 743″ to 99″ and 212″, respectively. As the deposition time further increases to 120 s, the FWHM value of ($10\bar{1}2$) decreases to 171″, however, the FWHM value of (0002) is basically unchanged, maintaining at a low level of 90–100″. The FWHM values of (0002) and ($10\bar{1}2$) rocking curve correlate with the screw dislocation density and the edge dislocation density, respectively [10]. The reduction of (0002) and ($10\bar{1}2$) FWHM values in the sample indicates that both screw and edge dislocation densities decrease. It has been reported that the dislocations can terminate or bend at SiN_x mask [11]. Therefore, the decrease of screw and edge dislocation density in the sample can be attributed to the blocking effect of SiN_x insertion mask to dislocation. Further, a longer deposition time can lead to a larger SiN_x-covering area and means that more dislocations are blocked. This is the reason that the FWHM value of ($10\bar{1}2$) further decreases as SiN_x deposition time increases from 30 s to 120 s. At the same time, the low-level and nearly constant FWHM value of (0002) indicates the screw dislocation density is enough low and it has been basically blocked by SiN_x mask. In addition, when the deposition time of SiN_x is longer than 120 s, the surface of sample becomes very rough [shown in the inset of Fig. 2(a)] because the regrown GaN film cannot coalesce. Therefore, we can decide that the optimum deposition time of SiN_x insertion mask for N-polar GaN is 120 s. Fig. 2(b) shows the peak positions of Raman spectra E_2(high) mode for GaN films in series I. In the relaxed bulk GaN, the E_2(high) mode peak position is 568 cm^{-1}[12]. Relative to the peak position of relaxed GaN, the peak positions of all the samples in series I show red shift. Moreover, the peak position of E_2(high) mode gradually closes to 568 cm^{-1} with disposition time of SiN_x increasing. The peak shift of E_2(high) mode is mainly influenced by strain and it can be used as an indicator for the strain state in the film [13]. The red shift of E_2(high) mode suggests that all the samples in series I are affected by tensile stress. Furthermore, the change of peak position indicates the tensile residual stress in GaN film decreases with the increase of SiN_x deposition time. This changing trend is same as that of

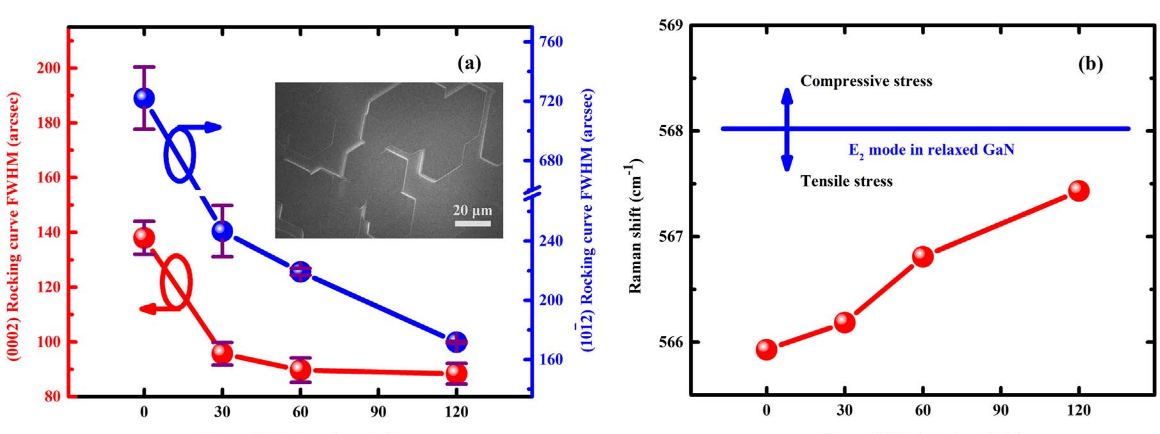

Fig. 2. XRD rocking curves FWHMs (a) and peak positions of Raman spectra E_2(high) mode (b) of N-polar GaN films with SiN_x insertion mask depending on the deposition time of SiN_x mask. Insert in (a) shows SEM image of the surface morphology of N-polar GaN film with SiN_x deposition time of 180 s.

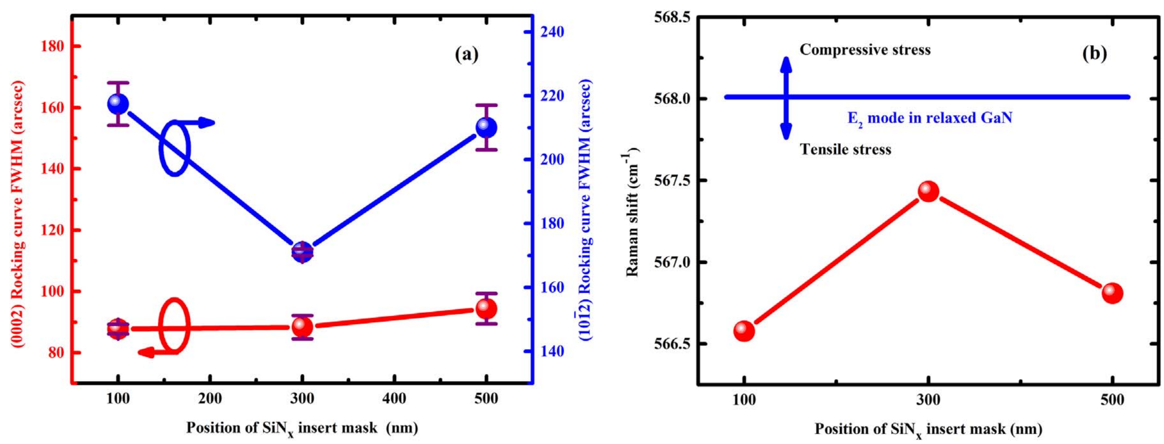

Fig. 3. XRD rocking curves FWHMs (a) and peak positions of Raman spectra E_2(high) mode (b) of N-polar GaN films with SiN_x insertion mask depending on the deposition position of SiN_x mask.

the FWHM value of (10$\bar{1}$2) XRD rocking curve. Therefore, we conclude that the tensile residual stress in GaN films can be effectively relaxed by reducing the density of edge dislocation. A similar result has also been demonstrated by other group [14].

Fig. 3(a) shows the FWHM values of XRD rocking curves of GaN in series II. The lowest FWHM value of (10$\bar{1}$2) is obtained in the sample, the SiN_x mask of which is inserted after the growth of 300 nm GaN, named as Sample B. However, the FWHM values of (0002) are nearly the same in the three samples with SiN_x insertion in different position. The FWHM values of (0002) and (10$\bar{1}$2) of Sample B are 88″ and 172″, respectively. Moram et al. [10] showed that the FWHM values of (0002) and (10$\bar{1}$2) rocking curves could be described as following equations:

$$\beta_{(0002)}=\beta_s \quad (1)$$

$$\beta^2_{(10\bar{1}2)}=(\beta_s cos43.\ 19)^2+(\beta_e sin43.\ 19)^2 \quad (2)$$

where β_s and β_e are the contributions of screw and edge dislocations to FWHM values of rocking curves. If the TDs are randomly distributed, the density of TDs can be calculated by the following equation:

$$\rho_s=\beta_s^2/4.\ 35b_s^2 \quad (3)$$

$$\rho_e=\beta_e^2/4.\ 35b_e^2 \quad (4)$$

where ρ_s and ρ_e are the densities of screw and edge dislocations, b_s and b_e are the Burgers vectors of screw and edge dislocations, respectively. According to Eqs. (1–4), the densities of screw and edge dislocations are estimated and listed in the Table 1. Compared to that of Sample A, the N-polar GaN sample without SiN_x mask, the screw and edge dislocations densities of Sample B reduce by 2.4 and 20 times, respectively. Fig. 3(b) shows the peak positions of Raman spectra E_2(high) mode for GaN films in Series II. The peak position of Sample B has the smallest red-shift value in Series II, which means that the least tensile residual stress exists in Sample B. This result is consistent with the consequence of the edge dislocation density. To better appreciate the stress state in the film, the stress value σ is calculated by the following equation [15]:

$$\Delta\omega = k\sigma$$

where Δω is the peak shift value of Raman spectra, and k is the stress factor. The residual stress results for all samples involved in this article are listed in the Table 1. According to above discussion, the optimum position of SiN_x for N-polar GaN films is inserting it after growth of 300 nm GaN film.

Table 1
The list of dislocation density and residual stress results for all samples.

SiN_x mask position/nm	SiN_x mask growth time/s	Screw dislocation density/cm^{-2}	Edge dislocation density/cm^{-2}	Residual stress/GPa
–	–	3.8×10^7	5.8×10^9	0.33
300	30	1.8×10^7	6.4×10^8	0.29
300	60	1.6×10^7	5.0×10^8	0.19
300	120	1.6×10^7	2.9×10^8	0.09
100	120	1.8×10^7	4.5×10^8	0.23
500	120	1.5×10^7	4.9×10^8	0.19

Temperature dependent Hall measurements were carried out to compare the electrical characteristic of Sample A and B. As shown in Fig. 4(a), the electron concentration of Sample A is temperature-independent, which suggests that Sample A is a degenerate semiconductor. However, Sample B shows a lower electron concentration and a classic donor freeze-out effect. It has been reported that the dominated impurity in N-polar GaN is oxygen atoms, which can substitute for nitrogen sites and act as shallow donors [5]. The TDs can be served as diffusion paths of oxygen from Al_2O_3 substrate [16]. Therefore, we think that the decrease of electron concentration in Sample B might be attributed to the reducing of unintentional doped oxygen concentration, which is caused by the lessening of threading dislocation density. Fig. 4(b) shows temperature-dependent Hall mobilities of these two samples. Sample B has a higher mobility and its mobility decreases with the increase of temperature. However, the mobility of Sample A slowly increases with the change of temperature. The dominant scattering mechanisms for the carriers in GaN films can be divided into two type: phonon scattering, such as polar optical phonon scattering, acoustic phonon scattering and piezoelectric scattering, and defect scattering, such as ionized impurity and dislocation scattering [17]. The effect of phonon scattering increases with temperature increasing, while that of defect scattering decreases with temperature increasing [18]. According to the different variation trends of mobilities in two samples, we can speculate that the dominated scattering mechanisms of these two samples are different. In Sample A, the mobility increasing with the increase of temperature implies that the dominated scattering mechanism is defect scattering. The opposite change trend of mobility in Sample B means that the dominated scattering mechanism is phonon scattering. In above discussion, we have proved that the TDs density and ionized-donor concentration of Sample B are much fewer than these of Sample A. Therefore, we conclude that the change of dominated scattering mechanism in Sample B can be attributed to the decrease of defect scattering. At the same time, that is also the reason for a higher mobility in Sample B.

Fig. 5 shows the low temperature PL spectra of Sample A and B at 10 K. The spectrum of Sample A shows a UV band at 3.476 eV, attributed to donor-bound exciton emission [19]. However, in the

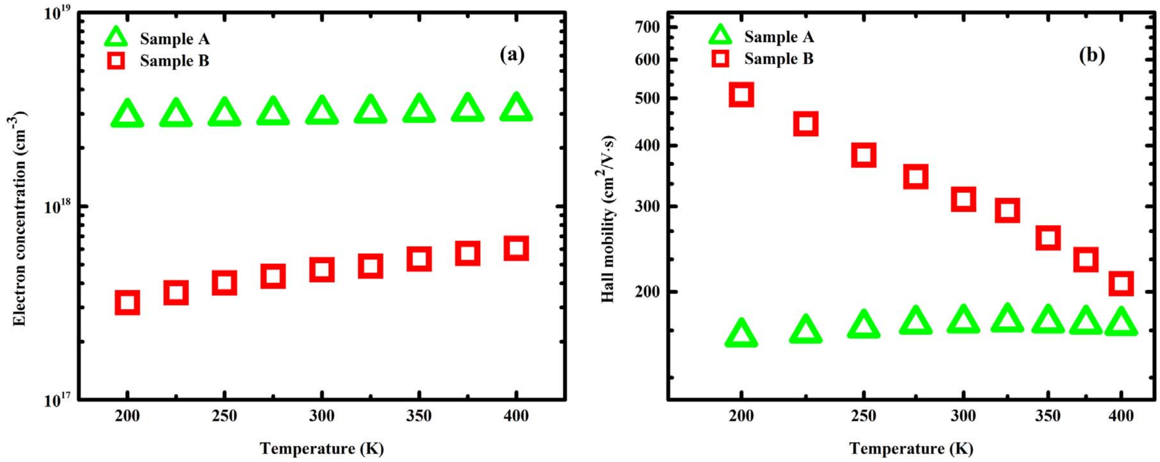

Fig. 4. Temperature dependent electron concentration (a) and Hall mobility (b) of Sample A and B.

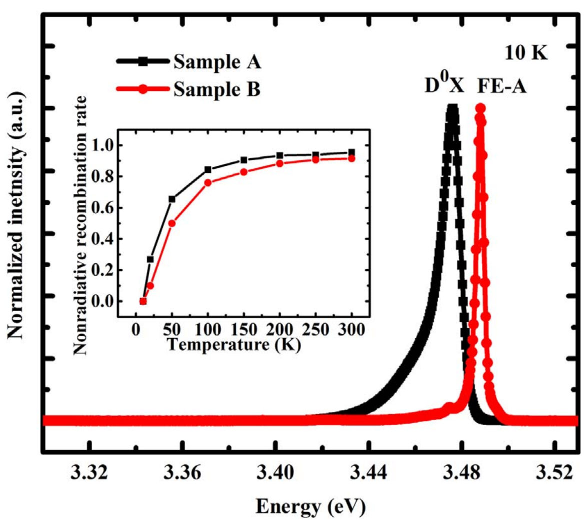

Fig. 5. Low temperature (10 K) PL spectra of Sample A and B. The inset shows the nonradiative recombination rate dependent on temperature.

spectrum of Sample B, a strong free-exciton transition presents at 3.488 eV. The appearance of free-exciton confirms the decrease of donor concentration in Sample B. In order to further compare the optical property, the nonradiative recombination rate is measured roughly by using the temperature dependence of the integrated PL intensity. At low temperature, the radiative recombination rate can be regarded as 100% [20]. Therefore, the radiative recombination rates of different temperature can be calculated by dividing the integrated PL intensity by that at 10 K. Nonradiative recombination rate can be obtained by using radiative recombination. As shown in inset of Fig. 5, Sample B has a lower nonradiative recombination rate. TD is a kind of nonradiative recombination center [21,22]. According to the XRD results, Sample B has a lower TDs density. So the decrease of nonradiative recombination rate in Sample B can be attributed to the reducing of the dislocation density, which is caused by SiN_x insertion mask.

4. Conclusions

In conclusion, we prove that the SiN_x insertion mask in N-polar GaN can suppress threading dislocations and relax the residual stress. By optimizing the position and deposition time of SiN_x insertion mask, high quality N-polar GaN film, with small FWHM values of (0002) and (10$\bar{1}$2) XRD rocking curve, was obtained. Hall measurements confirm the N-polar GaN film with SiN_x insertion mask has lower background carrier concentration and higher mobility. PL spectra show that the optical properties of N-polar GaN film with SiN_x insertion mask are improved observably.

Acknowledgments

This work was supported by the National Natural Science Foundation of China (Nos. 61274023, 61223005, 61376046 and 61674068), the National Key Research and Development Program (No. 2016YFB0400103), the Science and Technology Developing Project of Jilin Province (20150519004JH, 20160101309JC), and the Program for New Century Excellent Talents in University (NCET-13-0254).

References

[1] F. Akyol, D.N. Nath, S. Krishnamoorthy, P.S. Park, S. Rajan, Suppression of electron overflow and efficiency droop in N-polar GaN green light emitting diodes, Appl. Phys. Lett. 100 (2012) 111118.
[2] S. Keller, N.A. Fichtenbaum, M. Furukawa, J.S. Speck, S.P. DenBaars, U.K. Mishra, Growth and characterization of N-polar InGaN/GaN multiquantum wells, Appl. Phys. Lett. 90 (2007) 191908.
[3] S. Rajan, A. Chini, M.H. Wong, J.S. Speck, U.K. Mishra, N-polar GaN/AlGaN/GaN high electron mobility transistors, J. Appl. Phys. 102 (2007) 044501.
[4] Q. Sun, Y. Suk Cho, B.H. Kong, H. Koun Cho, T. Shine Ko, C.D. Yerino, I.-H. Lee, J. Han, N-face GaN growth on c-plane sapphire by metalorganic chemical vapor deposition, J. Cryst. Growth 311 (2009) 2948–2952.
[5] N.A. Fichtenbaum, T.E. Mates, S. Keller, S.P. DenBaars, U.K. Mishra, Impurity incorporation in heteroepitaxial N-face and Ga-face GaN films grown by metalorganic chemical vapor deposition, J. Cryst. Growth 310 (2008) 1124–1131.
[6] P. Vennéguès, B. Beaumont, V. Bousquet, M. Vaille, P. Gibart, Reduction mechanisms for defect densities in GaN using one- or two-step epitaxial lateral overgrowth methods, J. Appl. Phys. 87 (2000) 4175.
[7] D. Yang, H. Liang, Y. Qiu, S. Song, Y. Liu, R. Shen, Y. Luo, G. Du, Improvement of the quality of GaN epilayer by combining a SiNx interlayer and changed GaN growth mode, J. Mater. Sci.: Mater. Electron. 24 (2013) 2716–2720.
[8] J. Song, G. Yuan, K. Xiong, B. Leung, J. Han, Epitaxial lateral overgrowth of nitrogen-polar (000) GaN by metalorganic chemical vapor deposition, Cryst. Growth Des. 14 (2014) 2510–2515.
[9] D. Li, M. Sumiya, K. Yoshimura, Y. Suzuki, Y. Fukuda, S. Fuke, Characteristics of the GaN polar surface during an etching process in KOH solution, Phys. Status Solidi A 180 (2000) 357–362.
[10] M.A. Moram, M.E. Vickers, X-ray diffraction of III-nitrides, Rep. Prog. Phys. 72 (2009) 036502.
[11] A. Sagar, R.M. Feenstra, C.K. Inoki, T.S. Kuan, Y. Fu, Y.T. Moon, F. Yun, H. Morkoç, Dislocation density reduction in GaN using porous SiN interlayers, Phys. Status Solidi A 202 (2005) 722–726.
[12] H. Harima, Properties of GaN and related compounds studied by means of Raman scattering, J. Phys.: Condens. Matter 14 (2002) R967–R993.
[13] R. Kirste, M.P. Hoffmann, J. Tweedie, Z. Bryan, G. Callsen, T. Kure, C. Nenstiel, M.R. Wagner, Rn Collazo, A. Hoffmann, Z. Sitar, Compensation effects in GaN:Mg probed by Raman spectroscopy and photoluminescence measurements, J. Appl. Phys. 113 (2013) 103504.
[14] Y. Taniyasu, M. Kasu, T. Makimoto, Threading dislocations in heteroepitaxial AlN layer grown by MOVPE on SiC (0001) substrate, J. Cryst. Growth 298 (2007) 310–315.

[15] T. Kozawa, T. Kachi, H. Kano, H. Nagase, N. Koide, K. Manabe, Thermal stress in GaN epitaxial layers grown on sapphire substrates, J. Appl. Phys. 77 (1995) 4389.
[16] R. Jakiela, E. Dumiszewska, P. Caban, A. Stonert, A. Turos, A. Barcz, Oxygen diffusion into GaN from oxygen implanted GaN or Al_2O_3, Phys. Status Solidi C 8 (2011) 1513–1515.
[17] D.C. Look, R.J. Molnar, Degenerate layer at GaN/sapphire interface: influence on Hall-effect measurements, Appl. Phys. Lett. 70 (1997) 3377.
[18] M. Grundmann, The Physics of Semiconductors, 2nd ed, Springer, Heidelberg, 2010.
[19] G.D. Chen, M. Smith, J.Y. Lin, H.X. Jiang, S.-H. Wei, M. Asif Khan, C.J. Sun, Fundamental optical transitions in GaN, Appl. Phys. Lett. 68 (1996) 2784.
[20] P. Tao, H. Liang, X. Xia, Y. Liu, J. Jiang, H. Huang, Q. Feng, R. Shen, Y. Luo, G. Du, Enhanced output power of near-ultraviolet LEDs with AlGaN/GaN distributed Bragg reflectors on 6H–SiC by metal-organic chemical vapor deposition, Superlattices Microstruct. 85 (2015) 482–487.
[21] I. Yonenaga, S. Itoh, H. Makino, T. Goto, T. Yao, Photoluminescence of dislocations in plastically deformed GaN, Physica B 376–377 (2006) 455–459.
[22] J.Y. Shi, L.P. Yu, Y.Z. Wang, G.Y. Zhang, H. Zhang, Influence of different types of threading dislocations on the carrier mobility and photoluminescence in epitaxial GaN, Appl. Phys. Lett. 80 (2002) 2293.